JOURNAL OF GEOPHYSICAL RESEARCH, VOL. 112, C07029, doi:10.1029/2006JC003573, 2007

Nutrients dynamics in the southern Bay of Biscay (1993–2003): Winter supply, stoichiometry, long-term trends, and their effects on the phytoplankton community

Marcos Llope,[1,2] Ricardo Anadón,[1] Jorge Á. Sostres,[1] and Leticia Viesca[1]

Received 7 March 2006; revised 15 January 2007; accepted 2 May 2007; published 28 July 2007.

[1] The southern Bay of Biscay is a very active region in terms of hydrography due to the interannual variations of its Central Waters, the recurrence of mesoscale features such as slope currents and upwellings, and the freshwater discharges from land. This highly dynamic physical environment influences to a great extent the biogeochemical cycles of nutrients beyond the seasonal cycle typical of middle latitudes. By using a monthly time series (1993–2003) of nitrate, nitrite, phosphate, and silicate consisting of three stations placed along a cross-shelf transect, we assess the role of the physical forcing on nutrient seasonal and interannual dynamics within the upper 200 m, as well as the interactions with the biological component. The seasonal cycles of all nutrients and the stoichiometric balances (N:P and Si:N) are characterized along this coastal-oceanic gradient. The year-to-year variations in the extent of the winter replenishment are analyzed in relation to the background Central Waters and presence/absence of the Iberian Poleward Current. In the long term we report decreasing linear trends of nitrate, nitrite, and silicate as well as an uncoupled nonlinear variation (i.e., cyclical) for all nutrients. Furthermore, we investigate the effect of this complex long-term forcing on the phytoplankton: the linear trends are probably related to a decreasing primary production rate, while the nonlinear forcing may be responsible for controlling the community structure of phytoplankton.

Citation: Llope, M., R. Anadón, J. Á. Sostres, and L. Viesca (2007), Nutrients dynamics in the southern Bay of Biscay (1993–2003): Winter supply, stoichiometry, long-term trends, and their effects on the phytoplankton community, *J. Geophys. Res.*, *112*, C07029, doi:10.1029/2006JC003573.

1. Introduction

[2] The concentration of dissolved inorganic nutrients in the upper layers of the ocean is largely driven by biological activity. In temperate seas, the functioning of the biological pump together with the establishment of the seasonal thermocline lead to a net downward flux of nutrients during most of the year, while the winter deep mixing is responsible for their resupply from the subsurface reservoir, where the bulk of the export production is remineralized. Therefore the winter enrichment is of great importance as it sets the limits on the annual net primary production [*Koeve*, 2001; *Hydes et al.*, 2004].

[3] However, this picture is usually more complicated as other processes can alter these otherwise highly seasonal dynamics. Two mesoscale features, occurring at different times of the year, characterize the hydrography of the southern Bay of Biscay: the wind-driven upwellings and the Iberian Poleward Current (IPC) [*Llope et al.*, 2006]. Short-lived upwellings are frequent events inshore. The inflow of upwelled nutrients is especially important when it takes place in summer since the upper waters are almost depleted at that time. In contrast, the IPC is a winter current that conveys comparatively nutrient-poor waters (from subtropical origin) into the region, coinciding with the period of vertical mixing. The strength of this current varies from winter to winter and it can even be absent during some years [see *Llope et al.*, 2006, Figure 6]. Thus it is likely to affect the extent of the annual replenishment [*Álvarez-Salgado et al.*, 2003]. Apart from this, the occurrence of these two phenomena is known to have a structuring effect on the food web [*Fernández et al.*, 1993; *González et al.*, 2003] and as a result on the export efficiency of the biological pump [e.g., *Legendre and Rassoulzadegan*, 1996; *Azam*, 1998; *Legendre and Rivkin*, 2002].

[4] Nutrients in the Bay of Biscay and the northeastern coast of the Iberian Peninsula have been widely used so far as a quasi-conservative property of subsurface waters in order to estimate ageing and mixing of different water masses [*Pérez et al.*, 1993; *van Aken*, 2000a, 2000b]. Regarding their dynamics in the upper layers [*Tréguer et al.*, 1979], most of the studies have tended to focus on the

[1] Área de Ecología, Departamento de Biología de Organismos y Sistemas, Universidad de Oviedo, Uviéu/Oviedo, Spain.
[2] Now at Centre for Ecological and Evolutionary Synthesis, Universitetet i Oslo, Oslo, Norway.

0148-0227/07/2006JC003573$09.00

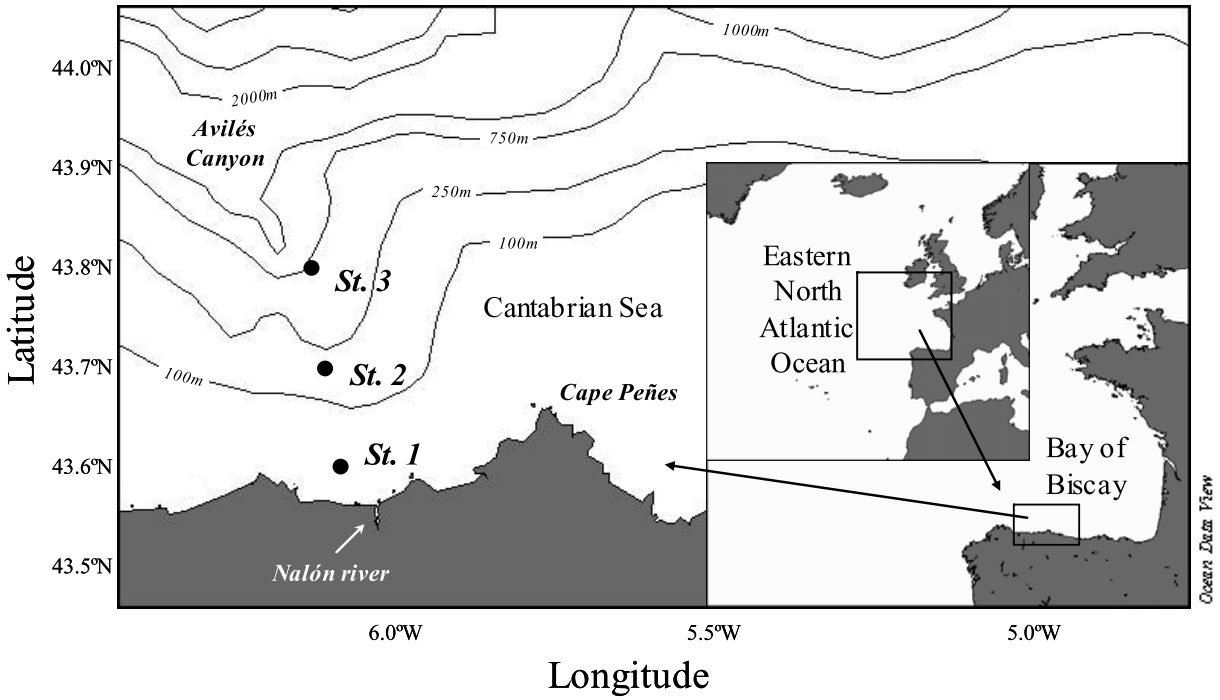

Figure 1. Sampling area. The Cantabrian Sea (south Bay of Biscay) showing the position of the three stations: Station 1 (St. 1), Station 2 (St. 2), Station 3 (St. 3), and the mouth of the Nalón River.

effect of mesoscale processes, such as IPC [*Gil*, 2003; *González-Quirós et al.*, 2004] and the coastal upwelling [*Botas et al.*, 1990; *Álvarez-Salgado et al.*, 2002]. However, there is little information on their seasonal and interannual variation from a long-term perspective.

[5] Time series data provide the necessary background information to collectively assess the importance of the physical and biological forcing in driving the nutrient dynamics [*Karl et al.*, 2001; *Lipschultz*, 2001]. However, available time series data from the Bay of Biscay and neighboring areas are primarily located close to the coast and therefore largely influenced by local topography (i.e., estuaries or rías) [see *Nogueira et al.*, 1997; *Soletchnik et al.*,. 1998] or are very shallow (L4 off Plymouth) [e.g., *Irigoien et al.*, 2000]. Thus, although they provide useful information on local processes, they are insufficient for a broader outlook.

[6] In this paper we aim to provide a comprehensive view of nutrient dynamics within the upper water column (0–200 m). We investigate the effect of the mesoscale processes on the seasonal and long-term dynamics as well as on the stoichiometric ratios (N:P and Si:N). To do this, we used the Asturian time series database which consists of three stations along a coastal-oceanic transect. This arrangement allows the assessment not only of the temporal but also the spatial extent of the above mentioned processes. A description of the hydrography for the same period (1993–2003) is given by *Llope et al.* [2006]. In this paper, the authors reported an increasing stratification of the upper layers and strong interannual variations of Central Waters. The implications of this long-term physical forcing are further investigated here on nutrients. Finally, a first attempt is made to explore any possible influence of this highly variable scenario on the productive capacity and taxonomic composition of phytoplankton.

2. Data and Methods

2.1. Study Area and Sampling Scheme

[7] The Cantabrian Sea is the southernmost part of the Bay of Biscay, in the eastern North Atlantic (Figure 1). The sampled area is locally influenced by the Nalón River, the most important Cantabrian River in terms of fresh water flux and nutrient loading into the southern Bay of Biscay [*Prego and Vergara*, 1998].

[8] Three permanent stations situated along a transect perpendicular to the coast (Figure 1) were sampled on a monthly basis from December 1992 to December 2003. Coastal Station 1 (Station 1; 43°36′N, 06°08′W, maximum depth 65 m) is 7 km offshore, Station 2 (43°42'N, 06°09'W, maximum depth 135 m) is a shelfbreak station (16.7 km) and Station 3 (43°46′N, 06°10′W, maximum depth 870 m) on the continental slope (23.4 km), is the most oceanic station. These stations are within the long-term monitoring program of the Instituto Español de Oceanografía (IEO, http://www.seriestemporales-ieo.net/). Nutrient concentrations were sampled at discrete depths in the water column by means of 5 L Teflon Niskin oceanographic bottles. Station 1 (St. 1) was sampled at 0, 10, 20, 30, 40, and 50 m, these same depths plus at 75 and 100 m at Station 2 (St. 2) and at 150 and 200 m at Station 3 (St. 3). Nutrient samples were subsequently frozen at −20°C for major nutrient analysis in the laboratory. Vertical profiles of temperature and salinity were collected from these stations

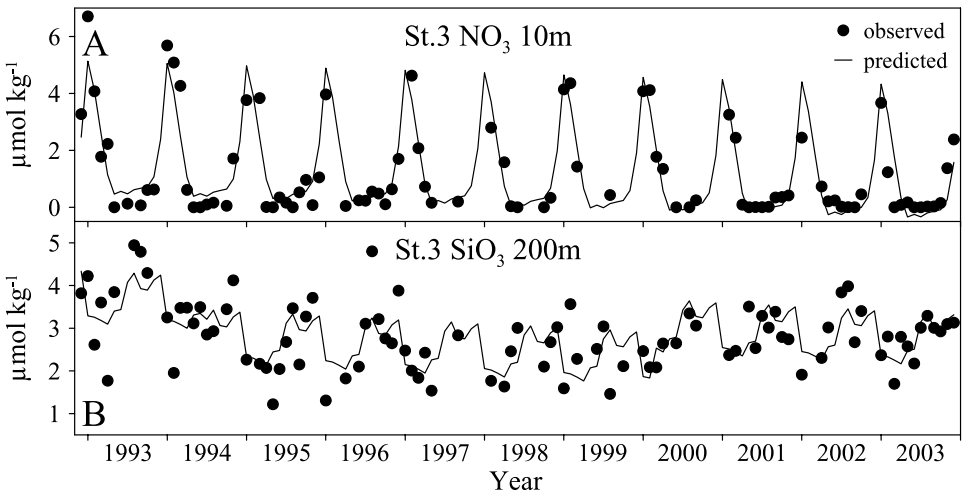

Figure 2. Example of model fit (observed versus predicted) for (a) surface nitrate and (b) deep silicate at the outermost station. The nitrate series showed a very seasonal pattern. Together with a long-term decreasing trend, these two components explained more than 80% of the variance. The silicate series showed a more complicated structure where apart from the seasonality and the general decreasing, trend the mean level shifted between high and low periods (note how the mean level changes with time).

at the same time that nutrients were sampled; see data and methods by *Llope et al.* [2006].

2.2. Nutrient Determination and Data Management

[9] Concentrations of nitrate [NO_3^-], nitrite [NO_2^-], phosphate [PO_4^{3-}], and silicate [$Si(OH)_4$] were determined according to the standard procedures of *Grasshoff et al.* [1983] using a Technicon AAII Autoanalyser (Industrial Method 158-71 W/A) and a Skalar SANplus (Skalar Analytical B.V.). Concentrations were corrected by water density at each sampling depth and are given in μmol kg^{-1}.

[10] The nitrogen to phosphorus (N:P) as well as the silicon to nitrogen (Si:N) atomic ratios were calculated taking into account both nitrate and nitrite concentrations (i.e., [NO_3^-] + [NO_2^-] : [PO_4^{3-}] and [$Si(OH)_4$] : [NO_3^-] + [NO_2^-]).

2.3. Phytoplankton Production and Taxonomic Composition

[11] Particulate organic carbon production rates were determined routinely (monthly, 1992–2003) for the middle station (St. 2) by means of simulated in situ incubations with ^{14}C following standard procedures (see detailed description of the method by *González et al.* [2003]).

[12] The 100 mL water samples for phytoplankton taxonomic determination were also routinely collected at three depths in the water column of the middle station (St. 2): at the surface, at the chlorophyll maximum depth and at the depth of the 1% of photosynthetic active radiation (PAR), and fixed in Lugol's iodine solution. At the laboratory, these were placed on composite sedimentation chambers, and subsequently observed under an inverted microscope Olympus IMT-2 using 40×, 100×, 150× and 400× magnifications. Abundances were estimated following the Utermöhl estimation method [*Utermöhl*, 1958]. A time series of the water column integrated abundances for 61 species were obtained from March 1995 to December 2003.

2.4. Time Series Analysis

[13] A central objective of time series analysis is to separate the deterministic structure of the data from the stochastic variability. Time series typically show a seasonal component, a long-term trend and a random or noise component [*Chatfield*, 1992]. To characterize the nature and importance of these components in the series of nutrients, we carried out dummy variable seasonal regression [*Cryer*, 1986], as this approach enables additive seasonal adjustment to be performed as part of the trend regression model and tolerates missing values. The trend was assumed to be linear and entered into the regression model as a sequential number (expressing time position from the first observation). The seasonal frame was built as a set of indicator (or dummy) variables and entered as independent regressors (as by *Llope et al.* [2006]). These variables assume the values of either 0 or 1; that is, the indicator for January takes a value of 1 in January and 0 for the rest of the year. We used 11 monthly indicators for 11 of the 12 months. The twelfth month is reserved as a baseline for comparison and computed afterward. Being ε_t the stochastic component, we may write the whole model as:

$$Y_t = a + bt + c_1 Jan_t + \ldots + c_{10} Oct_t + c_{11} Nov_t + \varepsilon_t \quad (1)$$

where a is the intercept, b is the slope of the trend and each of the c coefficients determines the effect of the month on the level of the series, i.e., the seasonal cycle.

[14] Once the model was fitted (see example in Figure 2), we checked that the residuals satisfied the regression assumptions. For the upper series of nitrate the distribution of residuals showed heteroscedasticity. To circumvent this problem we applied Weighted Least Squares (WLS) regression and compared these results with those from the

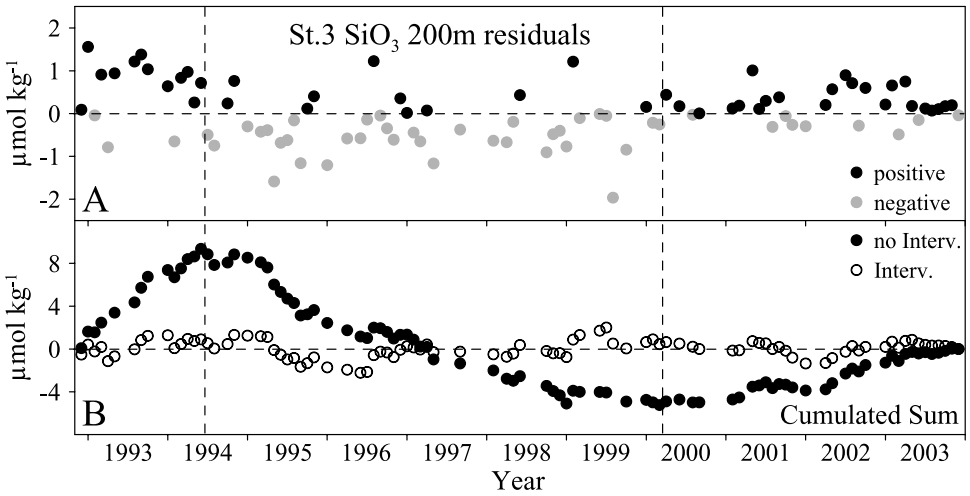

Figure 3. (a) Residuals of silicate at 200 m after extracting the seasonality and the linear trend (see the original series in Figure 2b). Three different periods can be seen: during the first and last period, the residuals were mainly positive (solid circles), while during the middle period they were predominantly negative (shaded circles). (b) The series of solid circles is the cumulated sum of the residuals shown above. This simple transformation makes the different periods much more evident and will be used later on for this purpose. The open circles are the residuals after applying the level shift intervention (i.e., after correction).

previous Ordinary Least Squares (OLS) regression. The former procedure yielded the same seasonal structure and distribution of trends. The difference was on the quantification of the trend slopes; these were about 2.5 times lower than those obtained with OLS. As WLS gives more importance to the less variable observations, these new trends are much more dependent on summer values, where nitrate levels are usually close to the detection limit. Considering this summer bias, we opted for OLS as carried out for the rest of the nutrients.

[15] To ensure that the models fully explained the dynamics of the nutrients, we looked for any remaining structure in the residuals. Far from being randomly distributed, all four nutrients showed periods of consecutive positive/negative anomalies (see Figure 3) indicating the existence of periods of high-/low-nutrient content over the defined seasonality and linear trends. This led to a further adjustment of the models by entering level shift interventions. This entailed the inclusion of other dummy series of length equal to the different period(s) where the residuals were mainly positive (or negative) to account for this change in level (see complete structure in Figure 2b). This procedure corrected this pattern in the residuals (see Figure 3b) but had little effect on the regression coefficients which were almost identical to those obtained without the intervention. In order to retain the comparability for the whole water column analysis, the previous results (i.e., without intervention) were kept and this long-term remnant variability is explicitly shown in a separate figure.

2.5. Stoichiometry

[16] To characterize the stoichiometric relationships between nutrients model II of the linear regression (aka geometric mean regression) was used [*Ricker*, 1984]. This regression technique describes the relationship between two observed variables without having to specify one as dependent on the other. The slope of the model II regression line (v) is defined as the ratio of the standard deviations of a bivariate sample:

$$v = \frac{S_y}{S_x} = \left(\frac{\sum y^2}{\sum x^2}\right)^{1/2} \quad (2)$$

The test statistic described by *Clarke* [1980] was applied to compare the slopes of the stoichiometric regression lines from different stations.

2.6. Multivariate Ordination

[17] The structure of the phytoplankton community was analyzed by means of nonmetric multidimensional scaling (MDS) [*Clarke and Warwick*, 1994]. This multivariate ordination technique is used to distribute samples in three dimensions (X, Y and Z axes) in such a way that the distances between pairs of samples reflect the extent to which these samples share particular species at comparable levels of abundance, i.e., the similarity of their biological communities. To include the temporal perspective into this spatial ordination the respective X, Y, and Z values were distributed over time and the resulting time series were analyzed as a proxy for community drift.

3. Results

3.1. Nutrient Seasonal and Vertical Variation

[18] Considering St. 3 as an ideal water body can help us to describe the seasonal dynamics of the different nutrients and the modifications occurring toward the coast. The virtually homogeneous concentration found in January for every nutrient and depth can be interpreted as the result of the mixed water column conditions at the beginning of the

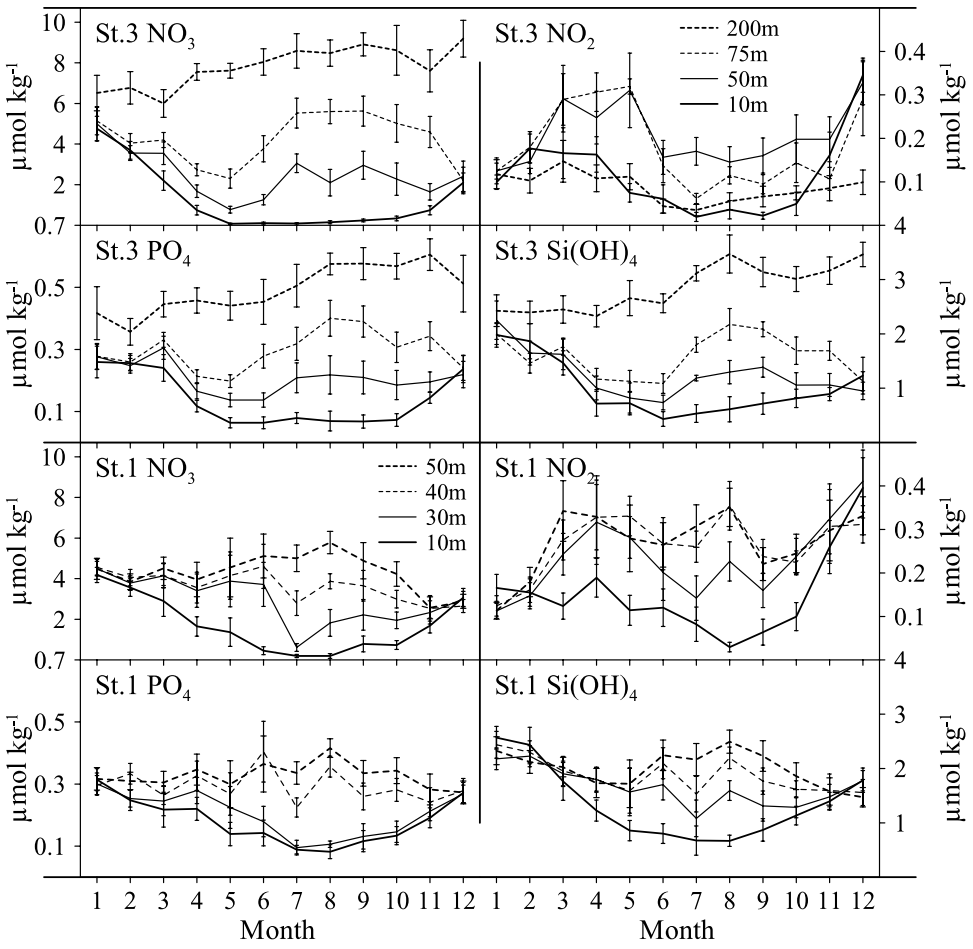

Figure 4. Seasonal cycles (mean and S.E.) of nitrate, nitrite, phosphate, and silicate at St. 3 and St. 1. Four depths are shown: 10, 50, 75, and 200 m for St. 3 and 10, 30, 40, and 50 m for St. 1. St. 2 (not shown) showed an intermediate pattern between these two stations.

year (Figure 4 (top)). Some months later, the thermal stratification brings about the typical upper layer depletion. Interestingly, the uppermost layer (10 m) decline in nutrients from January to May was not stepwise but continuous, and was also detected at middepths (50 and 75 m). From May onward, the middepth cycle diverged from that of the upper layer. The latter remained depleted until winter while at 50 and 75 m its concentration started to increase in June. At the deepest sampled depth (200 m) there was a continuous increase from January to the end of the year. A similar but much smoother seasonal pattern is seen on the coast (Figure 4 (bottom)) where the mixing processes have a much stronger effect, producing complete mixing as early as December.

[19] Nitrite showed quite a different pattern with a peak in the first half of the year, in particular at middepth, just at the same time as the rest of the nutrients were decreasing. It decreased during summer and increased again at the end of the year. In any case, the amount of nitrite was on average two orders of magnitude smaller than nitrate.

3.2. Long-Term Trends and Spatial Variability

[20] Except for phosphate, all the nutrients showed significant negative trends, although with different spatial (coast-ocean) and vertical (water column) distributions. Nitrate showed a general decreasing trend in the upper waters, affecting a thicker layer offshore and being much more limited to the surface toward the coast (Table 1). The trend of nitrite was more evenly distributed throughout the water column at St. 3 and St. 2 while it was only detected at the surface inshore (Table 2). No significant trends were detected for phosphate (Table 3). Finally, silicate trends were evenly vertically distributed offshore, but confined to the surface toward the coast (Table 4).

[21] In general, all nutrient species showed a relatively important seasonal component in terms of explained variability. However, the relative contribution of the seasonal component decreased toward the bottom and toward the coast to the extent that the deepest series at St. 1 and St. 2 usually lack any seasonality (Tables 1–4).

[22] Once the trend and the seasonal cycle were isolated, they were subtracted from the original series to get the residuals (i.e., the trend seasonally adjusted time series) and these were examined any remaining information (as shown in Figure 3). Far from being randomly distributed, they showed clear periods of consecutive positive/negative values, mainly driven by the deeper series and attenuated at the surface (where the seasonal component was much more

Table 1. Nitrate Long-Term Trends[a]

	Station 3				Station 2				Station 1			
		Slope				Slope				Slope		
	Seas, %	Percent	μmol kg^{-1} yr^{-1}	p Value	Seas, %	Percent	μmol kg^{-1} yr^{-1}	p Value	Seas, %	Percent	μmol kg^{-1} yr^{-1}	p Value
0 m	*76.7*	*2.4*	*−0.080*	*0.004*	*71.0*	*3.1*	*−0.092*	*0.001*	*44.6*	*2.4*	*−0.089*	*0.046*
10 m	*78.7*	*2.5*	*−0.081*	*0.002*	*74.0*	*3.1*	*−0.093*	*0.001*	52.7	-	−0.033	0.412
20 m	*73.7*	*3.3*	*−0.094*	*0.001*	*72.6*	*1.9*	*−0.068*	*0.011*	41.1	-	−0.024	0.608
30 m	*69.3*	*3.5*	*−0.099*	*0.002*	50.8	-	−0.040	0.287	25.6	-	−0.033	0.582
40 m	*55.9*	*3.5*	*−0.102*	*0.011*	26.1	-	−.0043	0.372	-	-	−0.051	0.391
50 m	*39.3*	*5.8*	*−0.131*	*0.005*	19.0	-	−.0029	0.573	-	-	−0.022	0.742
75 m	33.9	-	−0.059	0.282	22.6	-	−.0034	0.579				
100 m	27.9	-	−0.039	0.512	22.2	-	−0.004	0.950				
150 m	30.9	-	−0.090	0.113								
200 m	-	-	−0.027	0.692								

[a]Seasonality (column "Seas", as fraction of total variance, r^2, accounted by the seasonal cycle in the regression model) and linear trends (column "Slope", fraction of variance, slope, and significance) for all depths and stations (either significant or not). Italics are used to emphasize those depths at which nitrate trends are significant (p value < 0.05). Note that the introduction of an intervention at 200 m revealed that there is a weak seasonality masked by the nonlinear long-term variation. The same does not hold at St. 1 deepest layers.

important) (see Figure 5). One would expect these periods to vary in phase for the different nutrients but surprisingly, this was not the case.

3.3. Upper Layer Stoichiometry

[23] The spatial gradient shown above in the long-term variability is also observed in the stoichiometry. Figure 6 shows the N:P and Si:N ratio for the upper 30 m at the three stations. When using all the data (January–December), the N:P regression lines were identical for all stations and the slope indistinguishable from that found at the deepest sampling depth (Table 5). However, when focusing on the stratified period (May–October) the two outer stations showed significantly lower N:P ratios (Table 6) while not such lowering occurred at the coastal station. During the winter the N:P ratio was very similar for all the stations although there were slight differences in the intercepts; there is a very small residue of nitrate (0.027 μg kg^{-1}) at St. 1 when phosphate is depleted, while it is phosphate which is in excess at St. 2 and St. 3 when there is no nitrate (0.021 and 0.055 μg kg^{-1}, respectively).

[24] In contrast, the year-round Si:N ratio showed a different spatial pattern (Figure 6 (right)): it was significantly higher at St. 2 throughout the year (see Tables 5 and 6) and especially during the stratification. During this period silicate and nitrate lacked correlation at St. 3. Winter ratios were similar to year-round ratios.

3.4. Preformed Winter Nutrients

[25] To assess the effect of the Iberian Poleward Current (IPC) on the winter replenishment, the T-S profiles were compared with the nitrate profiles during winters of different Central Waters. In January 1995, 1996, 2000, and 2003 water masses were of the Bay of Biscay Central Waters subtype (BBCW) [*Llope et al.*, 2006] (Figure 7a). Nitrate concentration was similar at all stations and centered at 3.83 ± 0.04 μmol kg^{-1} (Figure 7b, thin lines). The higher values observed at the bottom of some of the profiles were related to incomplete mixing (they were below a maximum value of Brunt-Väisälä frequency) and were not included in the calculations. In contrast, January 2002 (also under BBCW conditions) was characterized by an intense IPC flowing onto the continental shelf (Figure 7a, shaded points). This year, the current showed almost no cross-shelf mixing and clearly separated fresher coastal waters from shelf-oceanic waters that were associated with it. This hydrographic structure is reflected in the nitrate profiles. Coastal waters showed nitrate concentrations typical of BBCW while they were considerably lower offshore (Figure 7b, shaded lines). The IPC event of 1996 did not

Table 2. Nitrite Long-Term Trends[a]

	Station 3				Station 2				Station 1			
		Slope				Slope				Slope		
	Seas, %	Percent	μmol kg^{-1} yr^{-1}	p Value	Seas, %	Percent	μmol kg^{-1} yr^{-1}	p Value	Seas, %	Percent	μmol kg^{-1} yr^{-1}	p Value
0 m	*38.1*	*7.7*	*−0.011*	*0.001*	*31.5*	*5.1*	*−0.009*	*0.008*	*35.1*	*2.5*	*−0.007*	*0.053*
10 m	*45.4*	*7.2*	*−0.010*	*0.001*	*42.1*	*5.8*	*−0.010*	*0.002*	39.1	-	−0.005	0.210
20 m	*36.4*	*8.4*	*−0.010*	*0.002*	*40.0*	*3.8*	*−0.007*	*0.015*	26.9	-	−0.008	0.071
30 m	*30.6*	*5.6*	*−0.010*	*0.010*	22.3	-	−0.002	0.512	23.8	-	−0.005	0.263
40 m	-	*6.1*	*−0.010*	*0.017*	28.9	-	−0.002	0.519	19.1	-	−0.005	0.242
50 m	-	*7.6*	*−0.012*	*0.008*	*35.9*	*5.2*	*−0.011*	*0.006*	17.0	-	−0.005	0.283
75 m	44.3	-	−0.002	0.479	20.7	-	−0.005	0.246				
100 m	32.3	-	−0.006	0.152	*26.5*	*6.4*	*−0.011*	*0.005*				
150 m	*21.9*	*13.1*	*−0.011*	*0.000*								
200 m	-	*30.7*	*−0.013*	*0.000*								

[a]Seasonality (column "Seas", as fraction of total variance, r^2, accounted by the seasonal cycle in the regression model) and linear trends (column "Slope", fraction of variance, slope, and significance) for all depths and stations (either significant or not). Italics are used to emphasize those depths at which nitrite trends are significant (p value < 0.05). Note that seasonality at 50 m (St. 1) was marginally significant (p = 0.069).

Table 3. Phosphate Long-Term Trends[a]

	Station 3				Station 2				Station 1			
		Slope				Slope				Slope		
	Seas %	Percent	μmol kg^{-1} yr^{-1}	p Value	Seas %	Percent	μmol kg^{-1} yr^{-1}	p Value	Seas %	Percent	μmol kg^{-1} yr^{-1}	p Value
0 m	44.9	-	−0.003	0.215	44.3	-	<−0.001	0.931	19.0	-	<−0.001	0.457
10 m	52.6	-	−0.002	0.356	57.6	-	<−0.001	0.714	30.3	-	<−0.001	0.940
20 m	57.4	-	−0.001	0.715	50.9	-	−0.002	0.444	24.7	-	−0.002	0.569
30 m	51.8	-	−0.001	0.757	24.5	-	−0.003	0.406	-	-	−0.002	0.665
40 m	38.2	-	−0.002	0.436	-	-	−0.002	0.619	-	-	−0.003	0.423
50 m	18.0	-	−0.005	0.165	-	-	−0.003	0.341	-	-	<−0.001	0.962
75 m	22.0	-	−0.001	0.748	-	-	<−0.001	0.989				
100 m	28.4	-	−0.002	0.592	-	-	0.003	0.585				
150 m	18.8	-	−0.008	0.205								
200 m	19.9	-	−0.007	0.293								

[a]Seasonality (column "Seas", as fraction of total variance, r^2, accounted by the seasonal cycle in the regression model) and linear trends (column "Slope", fraction of variance, slope, and significance) for all depths and stations (either significant or not). No significant trend was found for phosphate at any depth or station. Note that seasonality at 50 and 150 m (St. 3) was marginally significant (p = 0.078 and 0.068, respectively).

lead to a spatial structure comparable to that of 2002, even though its effect was visible in the nitrate profile at St. 2 (50 and 75 m). Including these two values, the nitrate carried by the IPC was about 2.72 ± 0.07 μmol kg^{-1}.

[26] January nitrate profiles collected during the presence of the Eastern North Atlantic Central Water subtype (ENACW) [*Llope et al.*, 2006] showed greater interannual and vertical variability (Figure 8). All these were affected by the IPC flow to some extent. Again, deep enrichment was found related to incomplete mixing while surface high values were related to low salinity, most probably due to intense runoff. Both features were visible in 1994 (nitrate profile at St. 1 is shown to better illustrate this surface enrichment, particularly important toward the coast). No other physical singularities were found at middepths apart from those that could be caused by the IPC. In 1994 the core of the IPC (as salinity maximum) was located at 38 m coinciding with a relative minimum of nitrate detected at 40 m. In January 1997, nitrate was strikingly high offshore compared to the other years. Two IPC cores were detected by means of temperature in this month. In 1999 it showed one salinity core at St. 3 and two at St. 2, again related to relatively low nitrate at about the same depths.

[27] Silicate vertical profiles followed a similar pattern, i.e., lower values associated with the IPC, though less affected by the extent of the deep mixing (the enrichment of 1997 was less pronounced) and more dependent on river discharges (a more intense upper layer enrichment of 1994, data not shown). Nitrite and phosphate varied in a much more independent fashion.

3.5. Biological Implications of the Long-Term Forcing

[28] In order to make a preliminary assessment of the biological consequences of this changing chemical environment, additional analysis was undertaken of two biological series from the middle station (primary production and phytoplankton composition). The time series of primary production rate (Figure 9) was analyzed following the same procedures and showed a decreasing trend of −0.182 mg C m^{-2} h^{-1} yr^{-1}(after natural log transformation, p value < 0.001) as well as some seasonality (26.6%).

[29] The series of phytoplankton composition was explored by means of an ordination analysis. The resulting three-dimensional plot gave no clear picture (Figure 10a). However, when projecting each of the three axes onto a temporal scale we found that two of them (the Y and Z axes) accounted for some seasonal variation; that is, samples collected in the same month appeared closer as a result of having similar communities (Figure 10b). In contrast, the *X axis* described some long-term variation which matched with the accumulated anomalies of the N:P ratio at 100 m depth (Figure 10c). As can be appreciated, the progressive increase in the N:P ratio after mid-1996 (as a result of the positive/negative phase of nitrate/phosphate

Table 4. Silicate Long-Term Trends[a]

	Station 3				Station 2				Station 1			
		Slope				Slope				Slope		
	Seas %	Percent	μmol kg^{-1} yr^{-1}	p Value	Seas %	Percent	μmol kg^{-1} yr^{-1}	p Value	Seas %	Percent	μmol kg^{-1} yr^{-1}	p Value
0 m	*38.3*	*7.3*	*−0.068*	*0.001*	*66.3*	*2.5*	*−0.061*	*0.002*	*32.5*	*3.2*	*−0.076*	*0.028*
10 m	*43.6*	*3.5*	*−0.043*	*0.022*	*57.8*	*4.7*	*−0.066*	*0.000*	46.4	-	−0.019	0.351
20 m	*44.0*	*6.0*	*−0.055*	*0.002*	*57.9*	*3.7*	*−0.049*	*0.003*	31.9	-	0.003	0.899
30 m	*41.2*	*6.2*	*−0.056*	*0.002*	*40.2*	*3.4*	*−0.046*	*0.022*	16.8	-	0.003	0.888
40 m	*34.7*	*6.7*	*−0.057*	*0.003*	36.0	-	−0.020	0.311	-	-	−0.035	0.135
50 m	*31.3*	*8.3*	*−0.063*	*0.002*	-	-	−0.021	0.311	-	-	0.002	0.943
75 m	33.1	-	−0.017	0.334	-	-	−0.011	0.616				
100 m	*24.8*	*5.5*	*−0.046*	*0.014*	-	-	0.017	0.465				
150 m	*32.4*	*8.0*	*−0.057*	*0.002*								
200 m	*25.8*	*4.6*	*−0.051*	*0.023*								

[a]Seasonality (column "Seas", as fraction of total variance, r^2, accounted by the seasonal cycle in the regression model) and linear trends (column "Slope", fraction of variance, slope, and significance) for all depths and stations (either significant or not). Italics are used to emphasize those depths at which silicate trends are significant (p value < 0.05).

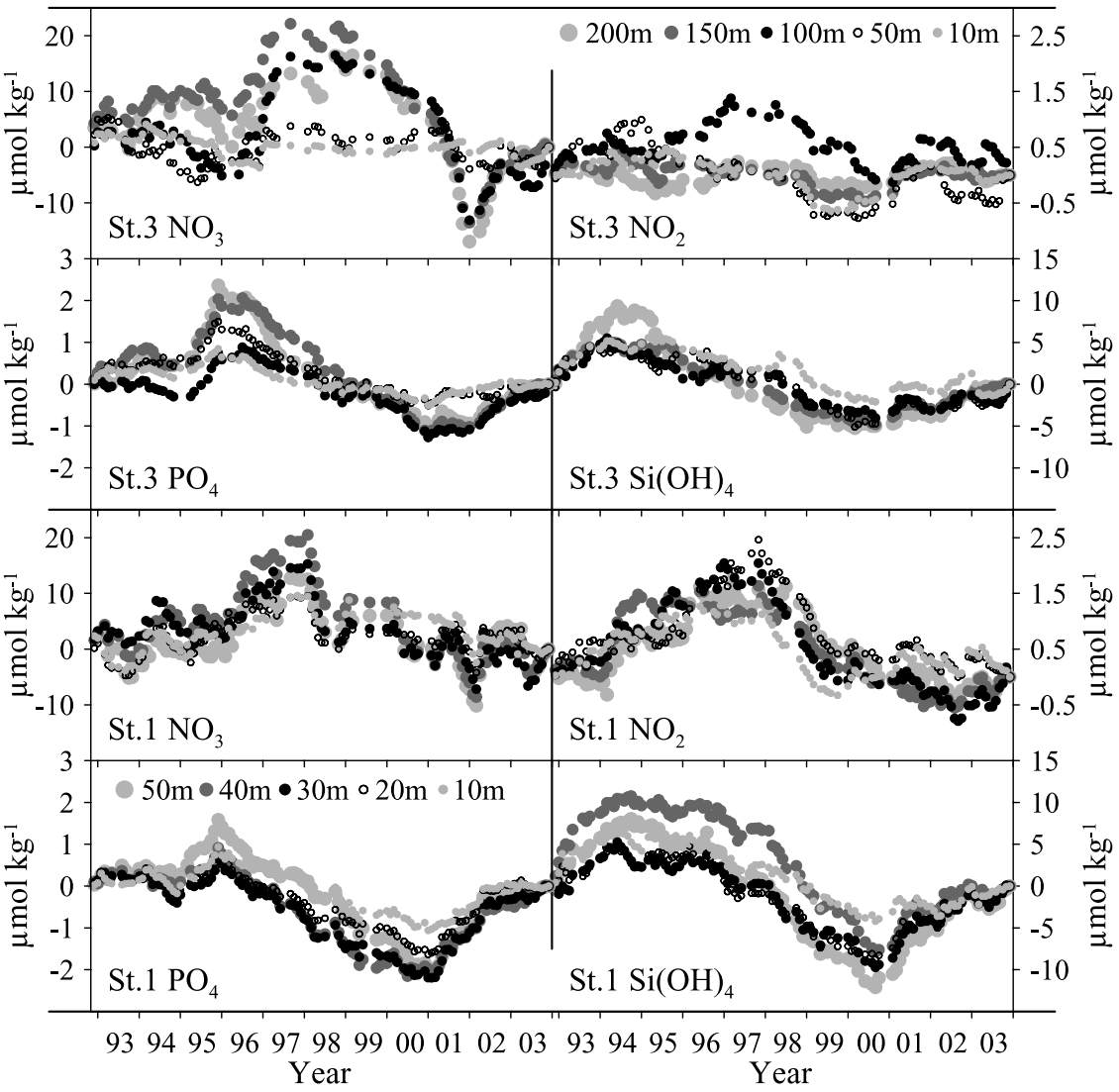

Figure 5. Cumulated sum of the residuals of nitrate, nitrite, phosphate, and silicate time series at 200, 150, 100, 50, and 10 m for St. 3 and at 50, 40, 30, 20, and 10 m for St. 1. The middle station showed an intermediate pattern (not shown).

(see cycles in Figure 5)) caused an unstable stoichiometric period around the end of 1997 which was followed by a period of fluctuating behavior of the X variation. Once the N:P ratio stabilized, the long-term community indicator reverted to a smooth temporal evolution.

4. Discussion

4.1. Winter Replenishment and the Annual Cycle

[30] Two main steps can be recognized in the winter mixing offshore (see Figure 4): a first upper mixing (0–75 m) in December and the deep mixing in January, although some hints of mixing can be seen already in October and November. The January replenishment led to an average increase of 100% for nitrate and 50% for silicate in the already rather mixed upper 75 m, corresponding to an equivalent decrease at 200 m. Although there must be remineralization below 200 m, the seasonal cycle appears to be fairly closed within this first 200 m. Inshore, the mixed period is much longer with little difference between the surface and the bottom layers for all nutrients from November to February.

[31] After the mixing, nutrient dynamics follow a marked seasonal pattern, especially at the surface. Our results showed a continuous removal of nutrients from January to May in contrast to a single and abrupt drop at the time of the spring bloom, as would have been anticipated according to the classical critical depth theory [*Sverdrup*, 1953]. This progressive removal of nutrients is observed above 75 m offshore (Figure 4). *Huisman et al.* [1999] described a mechanism based on critical turbulence through which phytoplankton can develop in well-mixed waters as winter blooms. It seems reasonable to attribute the observed nutrient decrease to the uptake by primary producers. Consequently, the whole period extending from winter to the spring bloom must be considered as very active in terms of phytoplankton growth and nutrient removal.

[32] Nitrite, which is an intermediary form between ammonium and nitrate, showed a different seasonal cycle. Its accumulation during winter suggests that mineralization

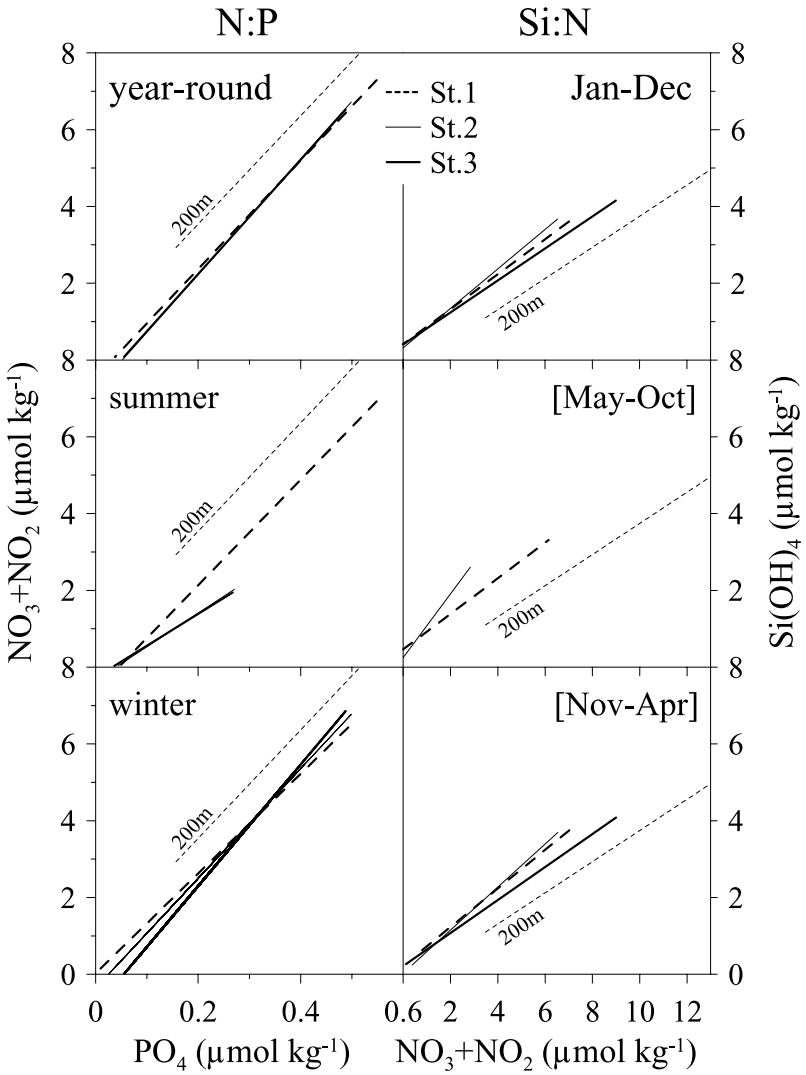

Figure 6. Model II linear regression lines for the averaged upper layer (left) N:P and (right) Si:N ratios. These ratios were estimated using the averaged concentration of nitrate + nitrite, phosphate, and silicate for the upper 30 m layer. The ratios are shown (top) for the whole year and for the (middle) summer and (bottom) winter seasons. The regression line of N:P and Si:N at 200 m is also shown as reference line.

is taking place. A second peak appeared in spring, this is probably the result of incomplete reduction of nitrate by phytoplankton during conditions of high nitrate and increasing light [*Lomas and Lipschultz*, 2006].

4.2. Cross-Shelf Variation of Nutrient Ratios

[33] The coastal effects (i.e., upwellings, river discharges, tides, and limited depth) influence nutrients to a great extent. Besides modifying the dynamics of the individual nutrient species, this forcing is also reflected in the stoichiometry (Figure 6). Many studies carried out in different areas of the ocean have repeatedly shown that there is a deficiency of nitrogen relative to phosphorus, according to the Redfield 16:1 ratio [*Tyrrell*, 1999, and references therein] and that the average N:P ratio for the world oceans below 500 m varies in reality around ~ 14.7 [*Falkowski et al.*, 1998; *Karl et al.*, 2001]. Our results show a N:P ratio at 200 m of 14.13 (see Table 5 and Figure 6). Although this ratio is likely to increase with depth, we assumed it to control to a great extent, the nitrate and phosphate replenishment of the upper layers. Coastal waters are not constrained overall by nitrogen limitation as they maintain a high N:P ratio during the stratification period, when the outer stations show a much lower ratio. This is the result of the pulsed but frequent delivery of nutrients by coastal

Table 5. Model II Regression Analysis of the Year-Round (Y-R) and May–October (M–O) N:P and Si:N ratios[a]

	Station 3		Station 2		Station 1		200 m	
	r	Slope	*r*	Slope	*r*	Slope	*r*	Slope
				N:P				
Y-R	0.762	14.9	0.702	15.04	0.601	14.13	0.291	14.13
M-O	0.553	8.27	0.672	8.78	0.716	13.75		
				Si:N				
Y-R	0.722	0.42	0.813	0.51	0.701	0.46	0.472	0.41
M-O	-	-	0.424	0.83	0.544	0.46		

[a]Slopes and Pearson's correlation are given for the three stations and the 200 m reference line. All shown Pearson's correlations were significant at 0.05 level.

Table 6. Comparison Among Stoichiometric Ratios[a]

	Year-Round		May–Oct.	
	St.2	St.1	St.2	St.1
		N:P		
St.3	0.921	0.611	0.713	*<0.001*
St.2	-	0.556	-	*<0.001*
		Si:N		
St.3	*0.022*	0.365	-	-
St.2	-	0.174	-	*0.001*

[a]Model II regression slopes are contrasted. Significantly different slopes are italicized. The test statistic used is described by *Clarke* [1980].

upwelling (see summer panel of Figure 6). In winter, it is the river discharges (richer in nitrate; e.g., see Figure 8 (top)) that cause nitrate to be relatively in excess (see intercepts in Figure 6).

[34] The Si:N dynamics proved to be decoupled offshore during summer (Figure 6). Moreover, the seasonal cycle of silicate was weaker at the oceanic than at the middle station (see Table 4) contrary to the pattern shown by the rest of the nutrients. Diatoms are known to be the primary users of silicate, as they need it to build their frustules [*Martin-Jezequel et al.*, 2000]. These algae dominate when high turbulence prevents them from sinking below euphotic zone. Such conditions can be frequently found toward the coast, even in summer, because of upwellings, but probably not offshore, where the summer stratification is much more persistent. Differences in the summer community structure between St. 3 and St. 2 together with different regeneration dynamics (associated with bottom depth) may explain both the uncoupled silicate-nitrate ratio and the relatively low seasonality of silicate offshore.

4.3. Long-Term Forcing and the Possible Biological Links

[35] The seasonality is the main force driving the series of nutrients in the long term (see variance decomposition in Tables 1–4). However, this picture does not tell the whole story. Actually, linear and nonlinear long-term forcing also plays an important part. Moreover, our results show how each nutrient species varies independently from the others in the long term. It is this uncoupled long-term variability that is of paramount importance regarding the future implications for the system.

[36] Negative linear trends were found for nitrate (along with nitrite) and silicate. Phosphate, which is supposed to regulate the primary productivity of the systems over longer timescales [*Tyrrell*, 1999], has not changed during the last decade. Regarding nitrate, the water column/spatial pattern of trends –comparable to a wedge with its thin end pointing toward the coast– resembles that shown by density in the area, but penetrating deeper into the water column [see *Llope et al.*, 2006, Table 3] and could therefore be linked to the ongoing increased stratification (Figure 11 (left)). In contrast, the water column decline of silicate requires a different explanation. As a consequence of their relatively large size, diatom production is linked to the generation of fast sinking particles, which plays a major role in exporting biogenic silica to deep ocean waters [*Smetacek*, 1998; *Tréguer and Pondaven*, 2000]. Besides, the dissolution of the latter is a slower process compared to the remineralization of N [*Sarmiento and Gruber*, 2006]. These two features of the silicate cycle if associated with a weaker/shallower winter mixing, either caused by relatively warmer winters or the Central Waters setting, could explain this water column trend. Finally, phosphate is known to have very high turnover rates [*Pomeroy*, 1960; *Vidal et al.*, 1999, and reference therein] because of its relatively easier release from organic matter, which may be one of the causes of this lack of trend.

[37] As put forward above, the concentration of nutrients in January may be considered the starting point of the annual biogeochemical cycle (see Figure 4). However, far from being regular, our results showed great interannual variation. The observed nutrient ratios following the winter replenishment varied from year to year, especially for nitrate

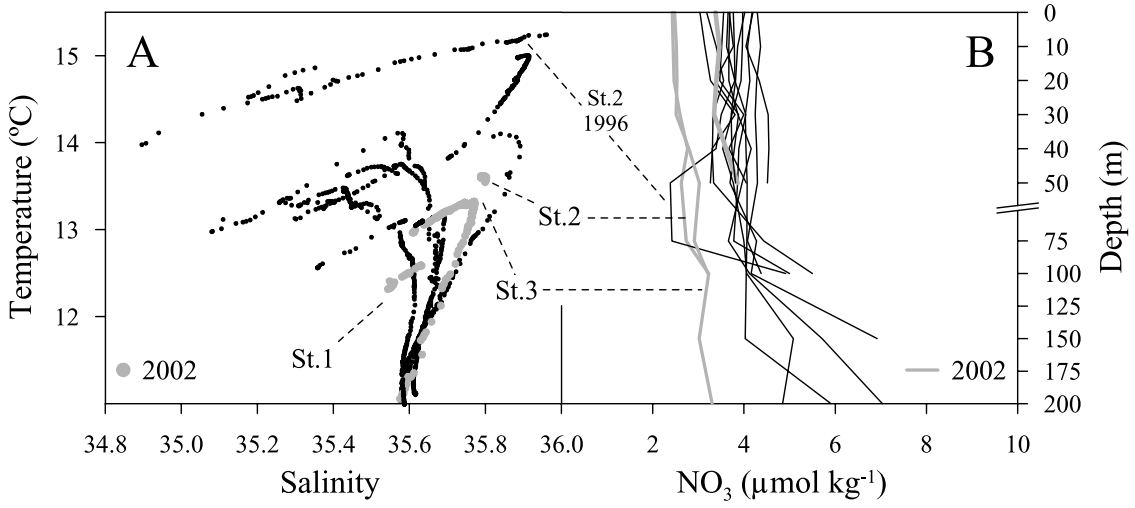

Figure 7. (a) Temperature-salinity (T-S) diagrams and (b) nitrate profiles in January 1995, 1996, 2000, and 2003 (thin points and thin lines) and 2002 (heavy shaded points and thick shaded lines). The three stations are shown together. Note that for St. 3 the T-S diagram characterizes the water column down to 500 m depth, while the nitrate profiles comprise only the first 200 m. There is no nitrate profile for January 2001, the other BBCW year according to *Llope et al.* [2006].

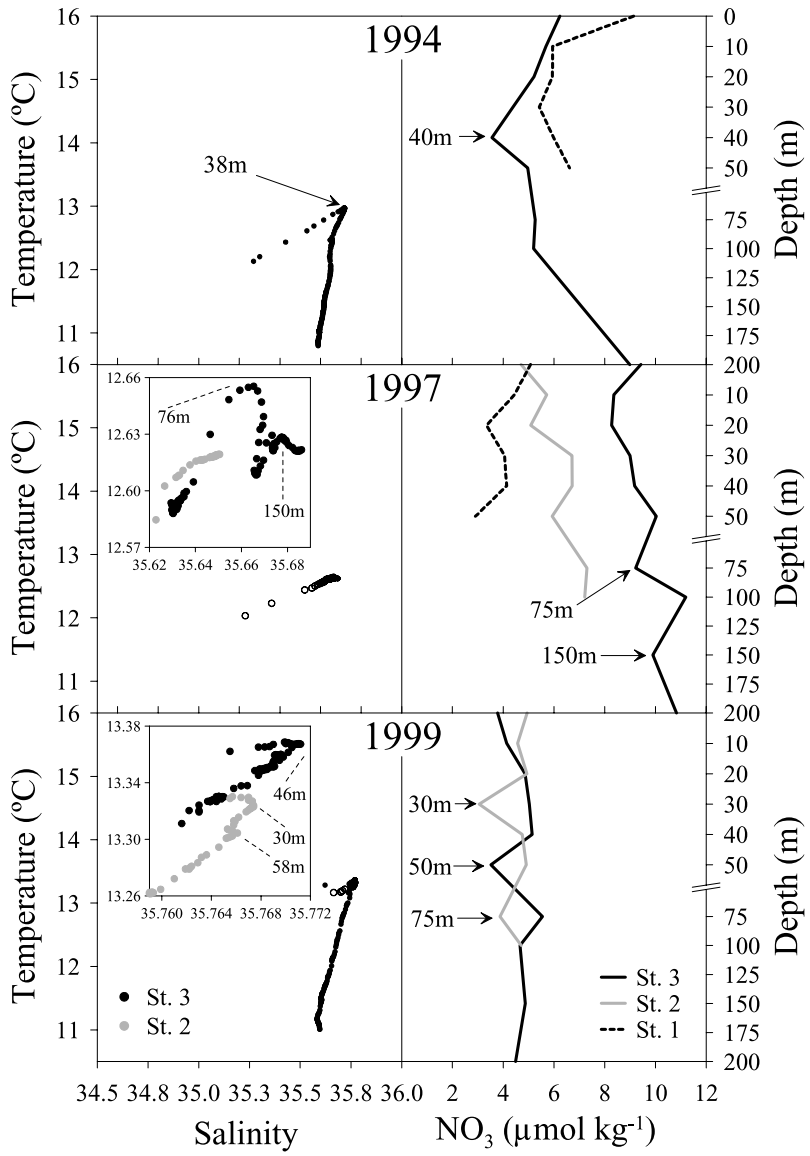

Figure 8. (a) Temperature-salinity diagrams and (b) nitrate profiles in January 1994, 1997, and 1999. T-S values are shown as solid circles for St. 3 and as shaded circles for St. 2. Nitrate profiles are shown as solid lines for St. 3, shaded lines for St. 2, and dashed lines for St. 1. The insets repeat the core of the IPC to show its structure in detail. Note that for St. 3 the T-S diagram characterizes the water column down to 500 m depth, while the nitrate profiles comprise the first 200 m.

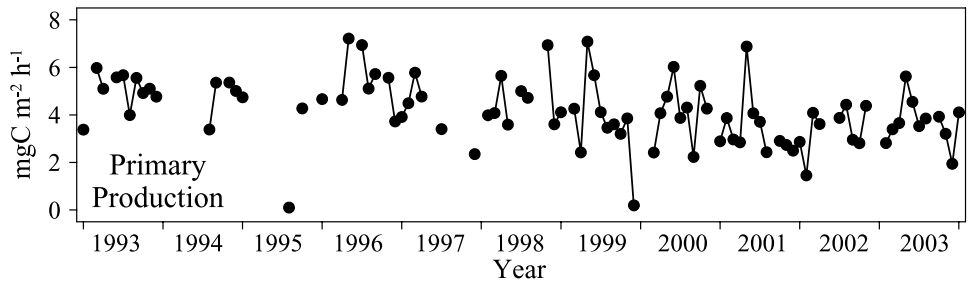

Figure 9. Evolution of primary production rate at St. 2 (log).

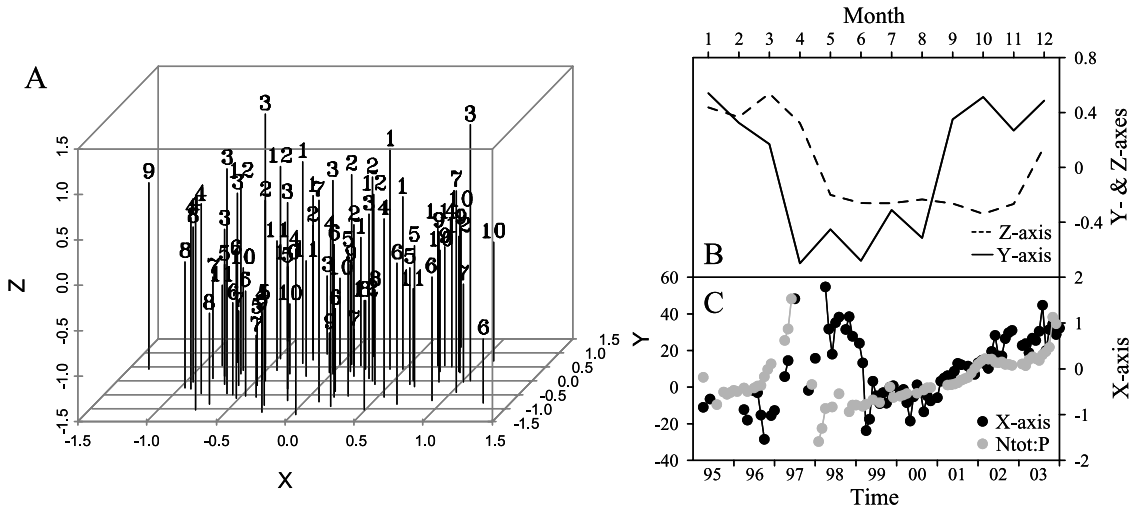

Figure 10. (a) Three-dimensional ordination of phytoplankton taxonomic samples (1995–2003) from MDS analysis (stress = 0.2) based on Bray-Curtis similarities calculated after fourth root transform of abundances. Sixty-one different species, those found in at least 10 samples, were included in the analysis. The numbers are the corresponding months of each sample. (b) The seasonal skeleton of the Y and Z axes (from seasonal regression analysis). This seasonal variability accounted for 65 and 38.5% of total variance, respectively. (c) Time projection of the X axis and the accumulated anomalies of the N:P ratio at 100 m (St. 2). Some of the values of the N:P ratio could not be shown to keep a suitable scale.

(e.g., the high values of 1997; see Figure 8), which points to the existence of other processes affecting nutrient concentrations/ratios. Silicate and phosphate showed less variability.

[38] The Iberian Poleward current conveys nutrient-poor waters of subtropical origin [*Frouin et al.*, 1990; *Haynes and Barton*, 1990], although on its way across the continental margins off Portugal and Galicia it mixes and gets progressively richer in nutrients. The values of nitrate given by *Álvarez-Salgado et al.* [2003] off Galicia during winter mixing (1.5–2.0 μmol kg^{-1}) are lower than those detected here ($\sim$2.8 μmol kg^{-1}) reflecting this progressive enrichment. From these observations we may conclude that the flow of the IPC reduces to a different extent the total winter supply (regarding nitrate and silicate) and that its

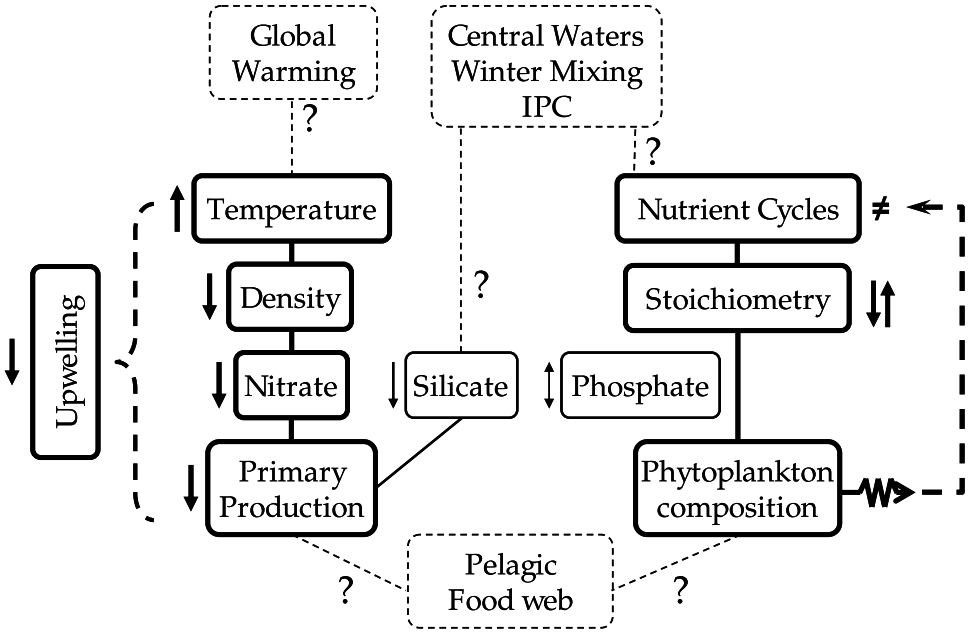

Figure 11. Possible links between the trends showed in the physical environment (from *Llope et al.* [2006]) and those described in this paper regarding nutrients and phytoplankton. The increasing temperature could be related to the decreasing density and nitrate since the distribution of trends (wedge shape) is very similar. This together with the relaxation of the upwellings could have contributed to the decrease seen in the primary production rate. On the other hand, the nutrient cycles and the related stoichiometric unbalances they bring about could have a structuring effect on the community of phytoplankton.

defertilizing effect may be enhanced when the BBCW signature occurs, since under such conditions the winter replenishment is on average weaker (Figures 6 and 7).

[39] All this hydrographic variability must be considered when trying to understand the causes behind the cycles shown in Figure 5. Although the mechanism is unclear, the hydrographic circumstances of a given year (depth of mixing, presence/lack of IPC, properties of the Central Water, runoff) can lead to unusual initial concentrations of a particular nutrient. This anomaly would propagate over a number of years, maybe with the feedback interplay of phytoplankton, resulting in the reported low-frequency cycles (Figure 11 (right)).

[40] Following up the nonlinear long-term forcing, all four nutrients showed periods of continuous positive anomalies, during which their respective concentrations were in excess compared to the mean level of the series, while others were characterized by a relative shortage. In addition, these cycles were out of phase with one another leading to the consequent fluctuation of stoichiometric ratios. According to Redfield, the balanced flow of N, P, and Si in and out of the biota leads to the universal stoichiometric ratio of 16:1:16 (for weakly silicified diatoms and other nondiatom phytoplankton the proportion of Si is much lower). Deviations from the latter are known to strongly influence phytoplankton communities [*Harris*, 1986; *Turner et al.*, 1998]. Therefore it is highly likely that the observed interannual variation had had some structuring effect on the local phytoplankton assemblage as suggested in analysis of the series of phytoplankton taxonomy (Figure 11).

[41] It is difficult to determine the exact way in which the phytoplankton community changes in relation to the physical-chemical conditions. Nevertheless, these results highlight the link between the environment and the biota, not only from a quantitative point of view (primary production) but also from a qualitative one (community structure). Moreover, these changes are likely to propagate upward, via bottom-up regulation, affecting the whole plankton community and ultimately marine renewable resources, as has already been reported for adjacent regions [*Aebischer et al.*, 1990; *Beaugrand et al.*, 2003]. A better understanding of the ways in which the environment influences marine food webs is crucial for an understanding of the regional impacts of global change [*Intergovernmental Panel on Climate Change*, 2001]. In this sense, this work makes a contribution regarding the current state and sensitivity of the southern Bay of Biscay shelfbreak region.

[42] **Acknowledgments.** This work was supported by a grant from the Ministerio de Ciencia y Tecnología (FPI Ph.D. fellowship), continued with a grant from the University of Oviedo (FTDOC-04) and a grant from the Ministerio de Educación y Ciencia (MEC postdoctoral fellowship). The Asturian time series sampling program was funded by the project Control a largo plazo de las condiciones químico-biológicas de la Plataforma Continental de Asturias (SV-02-IEO y SV-97-IEO-1) (Universidad de Oviedo, Instituto Español de Ocenografía) and Excelencia Investigadora del Principado de Asturias "Ecología de ecosistemas acuáticos" (PR-01-GE-3) 2001–2004. We would like to thank the many people whose efforts helped to establish and maintain the time series database presented here, especially those from the oceanographic group of the areas of ecology and zoology of the University of Oviedo as well as the whole crew of the oceanographic vessel *José Rioja*. We are especially grateful to L. Valdés, coordinator of the IEO time series program, for his continuous support to the Asturian section. It is thanks to all of them that this work has been possible. We thank W. Koeve, a referee whose comments improved an earlier version of this manuscript.

References

Aebischer, N. J., J. C. Coulson, and J. M. Colebrook (1990), Parallel long-term trends across four marine trophic levels and weather, *Nature*, *347*, 753–755.

Álvarez-Salgado, X. A., S. Beloso, I. Joint, E. Nogueira, L. Chou, F. F. Pérez, S. Groom, J. M. Cabanas, A. P. Rees, and M. Elskens (2002), New production of the NW Iberian Shelf during the upwelling season over the period 1982–1999, *Deep Sea Res., Part I*, *49*, 1725–1739.

Álvarez-Salgado, X. A., et al. (2003), The Portugal coastal counter current off NW Spain: New insights on its biogeochemical variability, *Prog. Oceanogr.*, *56*, 281–321.

Azam, F. (1998), Microbial control of oceanic carbon flux: The plot thickens, *Science*, *280*, 694–696.

Beaugrand, G., K. M. Brander, J. A. Lindley, S. Souissi, and P. C. Reid (2003), Plankton effect on cod recruitment in the North Sea, *Nature*, *426*, 661–664.

Botas, J. A., E. Fernández, A. Bode, and R. Anadón (1990), A persistent upwelling off the central Cantabrian Coast (Bay of Biscay), *Estuarine Coastal Shelf Sci.*, *30*, 185–199.

Chatfield, C. (1992), *The Analysis of Time Series: An Introduction*, 131 pp., CRC Press, Boca Raton, Fla.

Clarke, K. R., and R. M. Warwick (1994), *Change in Marine Communities: An Approach to Statistical Analysis and Interpretation*, Plymouth Mar. Lab., Plymouth, U. K.

Clarke, M. R. B. (1980), The reduced major axis of a bivariate sample, *Biometrika*, *67*, 441–446.

Cryer, J. D. (1986), *Time Series Analysis*, Duxbury, Boston, Mass.

Falkowski, P. G., R. T. Barber, and V. Smetacek (1998), Biogeochemical controls and feedbacks on ocean primary production, *Science*, *281*, 200–206.

Fernández, E., J. Cabal, J. L. Acuña, A. Bode, A. Botas, and C. García-Soto (1993), Plankton distribution across a slope current–induced front in the southern Bay of Biscay, *J. Plankton Res.*, *15*, 619–641.

Frouin, R., A. F. G. Fiúza, I. Ambar, and T. J. Boyd (1990), Observations of a poleward surface current off the coasts of Portugal and Spain during winter, *J. Geophys. Res.*, *95*, 679–691.

Gil, J. (2003), Changes in the pattern of water masses resulting from a poleward slope current in the Cantabrian Sea (Bay of Biscay), *Estuarine Coastal Shelf Sci.*, *57*, 1139–1149.

González, N., R. Anadón, and L. Viesca (2003), Carbon flux through the microbial community in a temperate sea during summer: Role of bacterial metabolism, *Aquat. Microbial Ecol.*, *33*, 117–126.

González-Quirós, R., A. Pascual, D. Gomis, and R. Anadón (2004), Influence of mesoscale physical forcing on trophic pathways and fish larvae retention in the central Cantabrian Sea, *Fish. Oceanogr.*, *13*, 351–364.

Grasshoff, K., M. Ehrhardt, and K. Kremling (1983), *Methods of Seawater Analysis,* 2nd ed., Chemie, Weinheim, Germany.

Harris, G. P. (1986), *Phytoplankton Ecology: Structure, Function and Fluctuation*, 384 pp., Chapman and Hall, London.

Haynes, R., and E. Barton (1990), A poleward flow along the Atlantic coast of the Iberian Peninsula, *J. Geophys. Res.*, *95*, 11,425–11,441.

Huisman, J., P. van Oostveen, and F. J. Weissing (1999), Critical depth and critical turbulence: Two different mechanisms for the development of phytoplankton blooms, *Limnol. Oceanogr.*, *44*, 1781–1787.

Hydes, D. J., R. J. Gowen, N. P. Holliday, T. Shammon, and D. Mills (2004), External and internal control of winter concentrations of nutrients (N, P and Si) in north-west European shelf seas, *Estuarine Coastal Shelf Sci.*, *59*, 151–161.

Intergovernmental Panel on Climate Change (2001), *Climate Change 2001: Impacts, Adaptation and Vulnerability: Contribution of Working Group II to the Third Assessment Report of the Intergovernmental Panel on Climate Change*, edited by J. J. McCarthy et al., 1032 pp., Cambridge Univ. Press, Cambridge, U. K.

Irigoien, X., B. Meyer-Harms, R. N. Head, R. P. Harris, D. Cummings, and D. Harbour (2000), Feeding selectivity and egg production of Calanus helgolandicus in the English Channel, *Limnol. Oceanogr.*, *45*, 44–54.

Karl, D. M., K. M. Björkman, J. E. Dore, L. Fujieki, D. V. Hebel, T. Houlihan, R. M. Letelier, and L. M. Tupas (2001), Ecological nitrogen-to-phosphorus stoichiometry at station ALOHA, *Deep Sea Res., Part II*, *48*, 1529–1566.

Koeve, W. (2001), Wintertime nutrients in the North Atlantic: New approaches and implications for new production estimates, *Mar. Chem.*, *74*, 245–260.

Legendre, L., and F. Rassoulzadegan (1996), Food-web mediated export of biogenic carbon in oceans: Hydrodynamic control, *Mar. Ecol. Prog. Ser.*, *145*, 179–193.

Legendre, L., and R. Rivkin (2002), Fluxes of carbon in the upper ocean: Regulation by food-web control nodes, *Mar. Ecol. Prog. Ser.*, *242*, 95–109.

Lipschultz, F. (2001), A time-series assessment of the nitrogen cycle at BATS, *Deep Sea Res., Part II*, *48*, 1897–1924.

Llope, M., R. Anadón, L. Viesca, M. Quevedo, R. González-Quirós, and N. C. Stenseth (2006), Hydrography of the southern Bay of Biscay shelf-break region: Integrating the multi-scale physical variability over the period 1993–2003, *J. Geophys. Res.*, *111*, C09021, doi:10.1029/2005JC002963.

Lomas, M. W., and F. Lipschultz (2006), Forming the primary nitrite maximum: Nitrifiers or phytoplankton?, *Limnol. Oceanogr.*, *51*, 2453–2467.

Martin-Jezequel, V., M. Hildebrand, and M. A. Brzezinski (2000), Silicon metabolism in diatoms: Implications for growth, *J. Phycol.*, *36*, 821–840.

Nogueira, E., F. F. Pérez, and A. F. Ríos (1997), Seasonal patterns and long-term trends in an estuarine upwelling ecosystem (Ría de Vigo NW Spain), *Estuarine Coastal Shelf Sci.*, *44*, 285–300.

Pérez, F. F., C. Mouriño, F. Fraga, and A. F. Ríos (1993), Displacement of water masses and remineralization rates off the Iberian Peninsula by nutrient anomalies, *J. Mar. Res.*, *51*, 869–892.

Pomeroy, L. R. (1960), Residence time of dissolved phosphate in natural waters, *Science*, *131*, 1731–1732.

Prego, R., and J. Vergara (1998), Nutrient fluxes to the Bay of Biscay from Cantabrian rivers (Spain), *Oceanol. Acta*, *21*, 271–278.

Redfield, A. C., B. H. Ketchum, and F. A. Richards (1963), The influence of organisms on the composition of seawater, in *The Sea*, vol. 2, edited by M. N. Hill, pp. 26–77, John Wiley, Hoboken, N. J.

Ricker, W. E. (1984), Computation and uses of central trend lines, *Can. J. Zool.*, *62*, 1897–1905.

Sarmiento, J. L., and N. Gruber (2006), Silicate cycling, in *Ocean Biogeochemical Dynamics*, edited by J. L. Sarmiento and N. Gruber, Princeton Univ. Press, Princeton, N. J.

Smetacek, V. (1998), Diatoms and the silicate factor, *Nature*, *391*, 224–225.

Soletchnik, P., N. Faury, D. Razet, and P. Goulletquer (1998), Hydrobiology of the Marennes-Oleron Bay: Seasonal indices and analysis of trends from 1978 to 1995, *Hydrobiologia*, *386*, 131–146.

Sverdrup, H. V. (1953), On conditions for the vernal blooming of phytoplankton, *J. Cons. Int. Explor. Mer*, *18*, 287–295.

Tréguer, P., and P. Pondaven (2000), Global change: Silica control of carbon dioxide, *Nature*, *406*, 358–359.

Tréguer, P., P. Le Corre, and J. R. Grall (1979), The seasonal variations of nutrients in the upper waters of the Bay of Biscay region and their relation to phytoplankton growth, *Deep Sea Res., Part A*, *26*, 1121–1152.

Turner, R. E., N. Qureshi, N. N. Rabalais, Q. Dortch, D. Justiæ, R. F. Shaw, and J. Cope (1998), Fluctuating silicate:nitrate ratios and coastal plankton food webs, *Proc. Natl. Acad. Sci. U.S.A.*, *95*, 13,048–13,051.

Tyrrell, T. (1999), The relative influences of nitrogen and phosphorus on oceanic primary production, *Nature*, *400*, 525–531.

Utermöhl, H. (1958), Zur Vervollkommung der quantitativen Phytoplankton-Methodik, *Mitt. Int. Ver. Limnol.*, *9*, 1–38.

van Aken, H. M. (2000a), The hydrography of the mid-latitude northeast Atlantic Ocean I: The deep water masses, *Deep Sea Res., Part I*, *47*, 757–788.

van Aken, H. M. (2000b), The hydrography of the mid-latitude Northeast Atlantic Ocean II: The intermediate water masses, *Deep Sea Res., Part I*, *47*, 789–824.

Vidal, M., C. M. Duarte, and S. Agustí (1999), Dissolved organic nitrogen and phosphorus pools and fluxes in the central Atlantic Ocean, *Limnol. Oceanogr.*, *44*, 106–115.

R. Anadón, J. Á. Sostres, and L. Viesca, Área de Ecología, Departamento de Biología de Organismos y Sistemas, Universidad de Oviedo, Catedrático Valentín Andrés Álvarez, E-33071 Uviéu/Oviedo, Spain.

M. Llope, Centre for Ecological and Evolutionary Synthesis, Universitetet i Oslo, P.O. Box 1066, Blindern, N-0316 Oslo, Norway. (marcos.llope@bio.uio.no)